Electronic Supplementary Information

Ferroelectric solar cells based on inorganic–organic hybrid perovskite

Bo Chen,*[a] Jian Shi,[b] Xiaojia Zheng,*[a] Yuan Zhou,[a] Kai Zhu,[c] Shashank Priya*[a]

a, Center for Energy Harvesting Materials and System, Virginia Tech, Blacksburg, Virginia 24061, United States

b, Department of Materials Science and Engineering, Rensselaer Polytechnic Institute, Troy, New York 12180, United States

c, Chemical and Nanoscience Center, National Renewable Energy Laboratory, Golden, Colorado 80401, United States

Corresponding author: bochen09@vt.edu, xiaojia@vt.edu, spriya@vt.edu

Experimental details:

Materials and Sample Preparation:

Preparation of $MAPbX_3$ Perovskite Solution: Methylamine (27.86 ml, 40% in methanol, TCI) and hydroiodic acid (30 ml, 57 wt% in water, Sigma-Aldrich) were mixed at 0°C and stirred for 2 h. The precipitate was recovered by evaporation at 50°C for 1 h. The methylammonium iodide (CH_3NH_3I) was washed with diethyl ether three times and finally dried at 60°C in a vacuum oven for 24 h. CH_3NH_3I and $PbCl_2$ (99.999%, Sigma-Aldrich) were dissolved in anhydrous N,N-Dimethylformamide (DMF) at a 3:1 molar ratio of CH_3NH_3I to $PbCl_2$, to produce a 40 wt% mixed halide perovskite ($MAPbI_{3-x}Cl_x$) precursor solution. The mixture solution was stirred at room temperature for 10 min just before using. For $MAPbI_3$ precursor, the prepared MAI and PbI_2 (Sigma-Aldrich) were added in a mixture of DMF and DMSO (7:3 v/v) for 0.8M; for $MAPbBr_3$ precursor, MABr powders (Lumtec) and $PbBr_2$ (Sigma-Aldrich) were added in a mixture of DMF and DMSO (7:3 v/v) for 0.8M $MAPbBr_3$ solution. The resulting $MAPbI_3$ and $MAPbBr_3$ precursor solutions were stirred overnight before using.

Preparation of the compact TiO_2 layer solution: 369 μL of titanium isopropoxide (99.99% Sigma-Aldrich) were added into 2.53 mL of ethanol, at the same time, 35 μL of a 2 M HCl solution were added into 2.53 mL of ethanol in another vial. The second solution was then added dropwise to the first solution and then stirring for 1 h. The mixture was filtered with a PFTE 0.2 μm filter.

Device Fabrication:

Fluorine-doped tin oxide (FTO) coated glasses (7Ω/sq, Sigma-Aldrich) used in this study were ultrasonically cleaned with acetone, ethanol and deionized water, and then dried with a nitrogen stream. The compact TiO_2 blocking layer was spin-coated on the FTO substrate at 2,000 rpm for 20 s using the mildly acidic titanium isopropoxide solution and heated at 500°C for 15 min. Either the bare FTO or FTO with 30 nm gold thin film was used as the substrate to deposit the mesoporous Al_2O_3 layer by spin-coating the diluted Al_2O_3 paste (Al_2O_3 paste (Sigma-Aldrich, 702129): ethanol=1:6 wt %) at 5000 RPM for 45 s. The Al_2O_3 layers were then sintered at 150°C for 30 minutes in air before using. $MAPbI_{3-x}Cl_x$ perovskite solution was spin-coated on the substrates (cp-TiO_2 coated FTO or mp-Al_2O_3 coated FTO) at 2000 rpm for 30 s, and then annealed at 90°C for 1 h and 100°C for 30 minutes in air. $MAPbI_3$ (or $MAPbBr_3$) perovskite solutions were coated onto the substrate by a two-step spin-coating process at 1,000 rpm for 10 and 4,000 rpm for 20 s, respectively. At the end of the second spin-coating step, the substrate was treated with toluene drop-casting. The obtained samples were dried on a hot plate at 100 °C for 10 min in glove box. Finally, 100 nm of gold was thermally evaporated on the perovskite film. The active area of each device was 0.1 cm^2.

Characterization:

Piezoelectric force microscopy (PFM) was performed using a scanning probe station (Bruker Dimension Icon, USA) with conductive Platinum-Iridium coated tip (SCM-PIT, Bruker). All the piezoelectric phase mappings were conducted under resonance-enhanced mode. In order to investigate the polarization switching behavior of domains, either a positive or negative DC bias was applied using the scanning tip on the specimen. For local hysteresis loop measurement, the out-of-plane piezoelectric response was measured at selected locations on the ferroelectric film surface as a function of DC bias superimposed on the AC modulation bias. The AC drive amplitude was 1000 mV (~300 kHz) during the DC bias sweep.

Photovoltaic performance of the solar cells were analyzed under one sun (AM 1.5G, 100 mW/cm^2) illumination with a solar simulator (150 W Sol 2A^{TM}, Oriel). During the measurement, different bias voltages were applied on the solar cell for 10 s to pole the perovskite thin film, and then solar cells were short circuited for 5 s after poling to avoid the effect of capacitive charging during the poling; subsequently, the current-voltage characteristics of each cell were recorded with a Keithley digital source meter (model 2400).

Scanning electron microscopy images were obtained from scanning electron microscopy (SEM, Quanta 600 FEG, FEI Company) operated at an accelerating voltage of 5 kV.

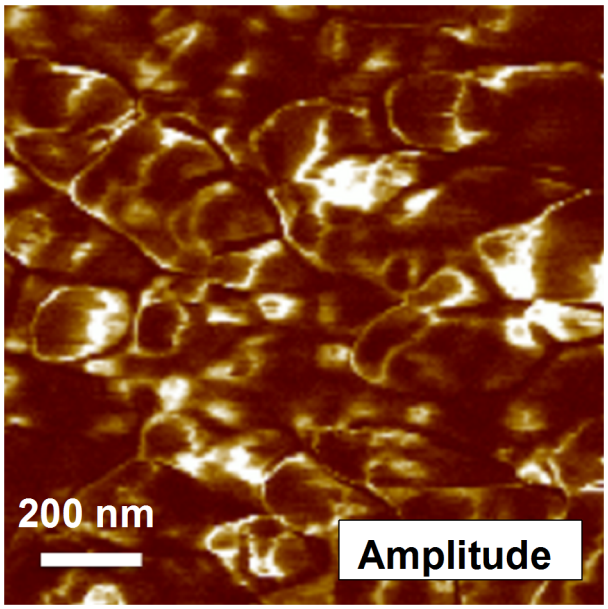

Fig. S1. PFM amplitude image of the as-grown $MAPbI_{3-x}Cl_3$ thin film in Fig. 1a.

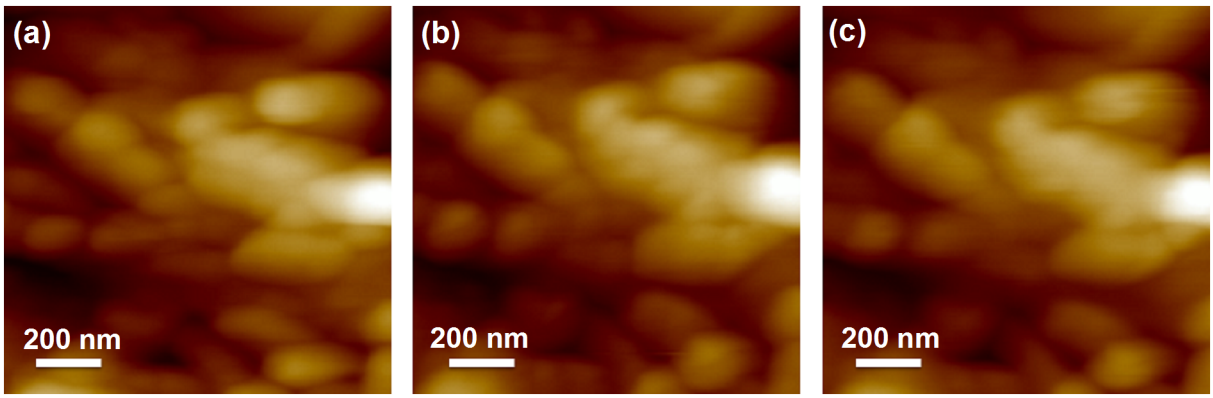

Fig. S2: PFM topology for the $MAPbI_3$ thin film after +5V poling, -5V poling, and +5V poling as shown in Fig 1d, e, and f, respectively.

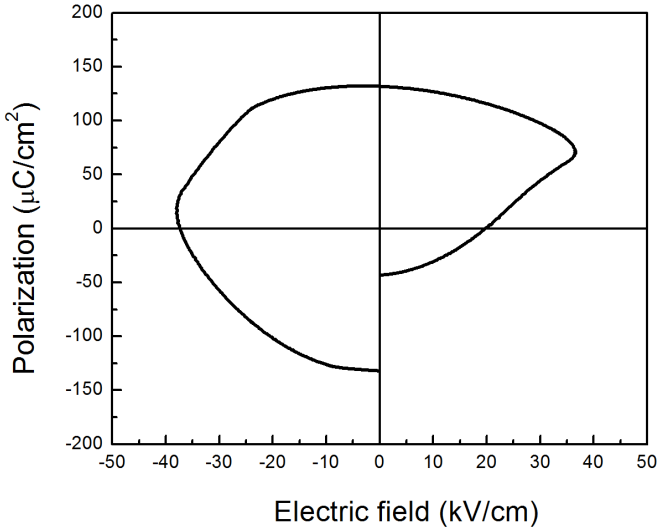

Fig. S3. Polarization-electric field (P-E) loop of $MAPbI_{3-x}Cl_x$ based on metal/FE/metal structure (FTO/Au/mp-Al_2O_3/$MAPbI_{3-x}Cl_x$/Au in Fig. 4d). The area of the top Au electrode is 0.1 cm^2.

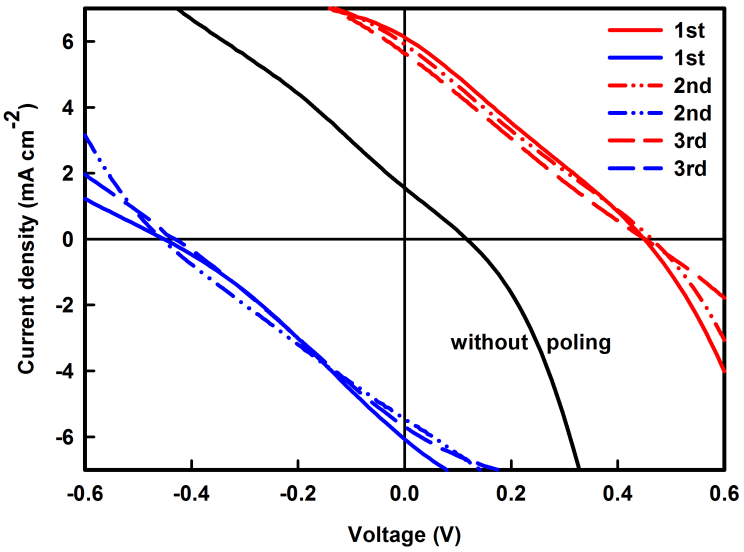

Fig. S4: The photovoltaic performance of the ferroelectric solar cell based on Au/$MAPbI_{3-x}Cl_x$/Au under repeat positive poling (red line) and negative poling (blue line).

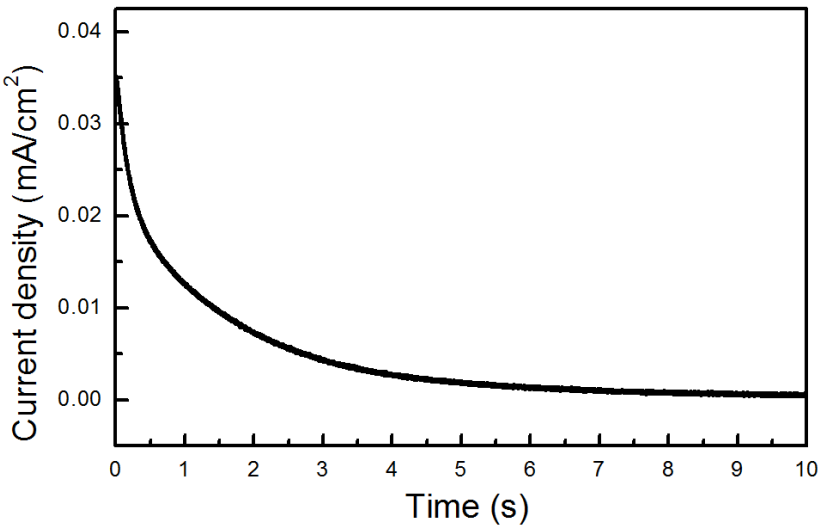

Fig. S5: The current flow of the Au/$MAPbI_{3-x}Cl_x$/Au ferroelectric solar cells after electric poling at -2V and then short circuit.

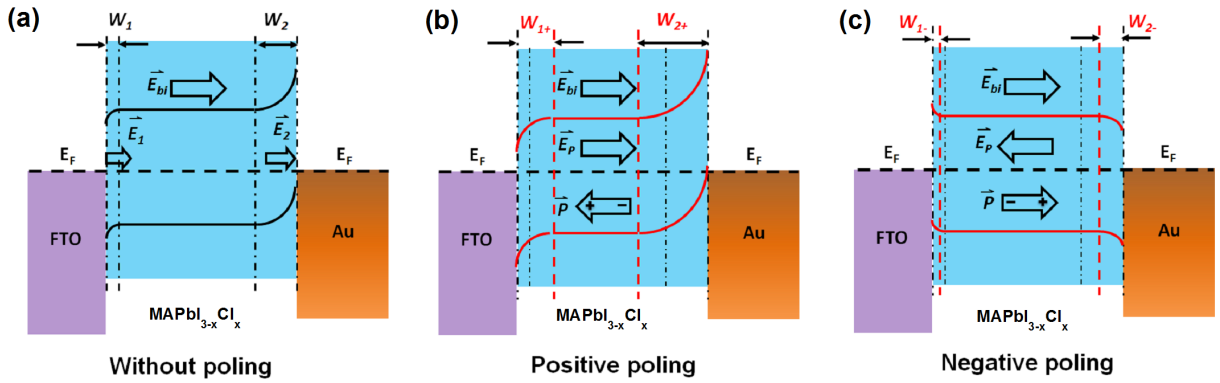

Fig. S6. Schematics of band diagram for ferroelectric solar cell based on FTO/mp-Al_2O_3/$MAPbI_{3-x}Cl_x$/Au under different polarization conditions: (a) without poling (b) after positive poling and (c) negative poling.

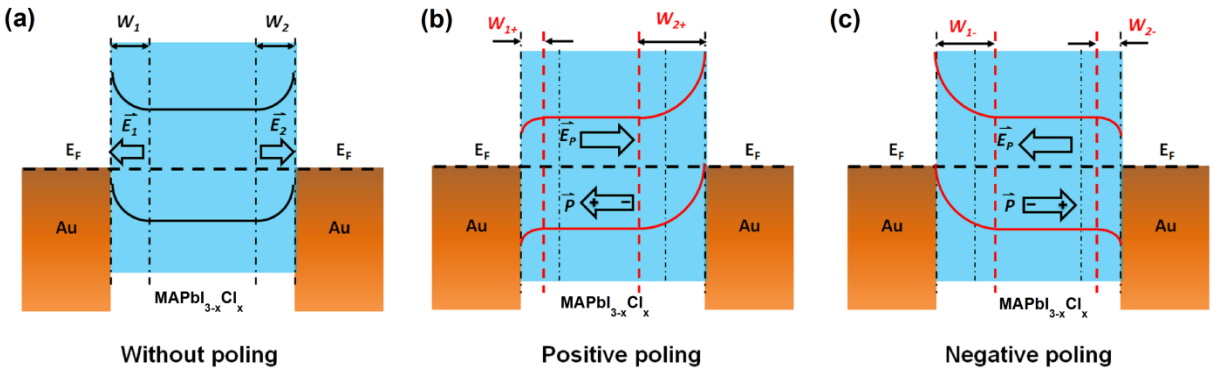

Fig. S7. Schematics of band diagram for ferroelectric solar cell based on FTO/Au/mp-Al_2O_3/$MAPbI_{3-x}Cl_x$/Au under different polarization conditions: (a) without poling (b) after positive poling and (c) negative poling.

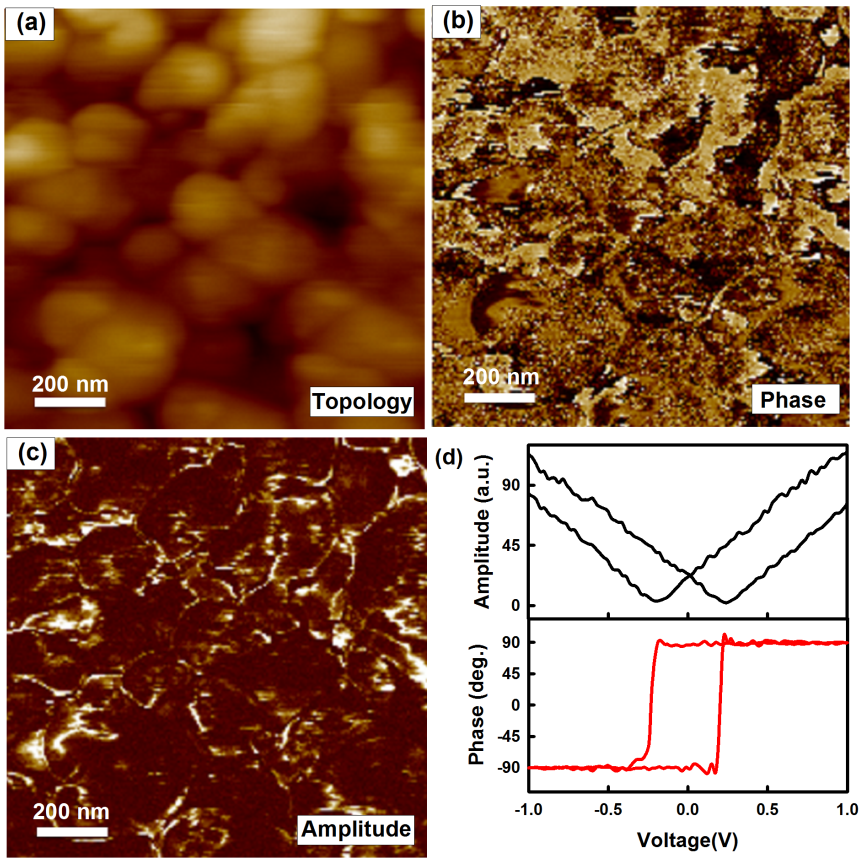

Fig. S8. (a) PFM topology, (b) PFM phase image, and (c) PFM amplitude image of the as-grown $MAPbI_3$ thin film. (d) Piezoresponse amplitude and piezoresponse phase at different bias voltages.

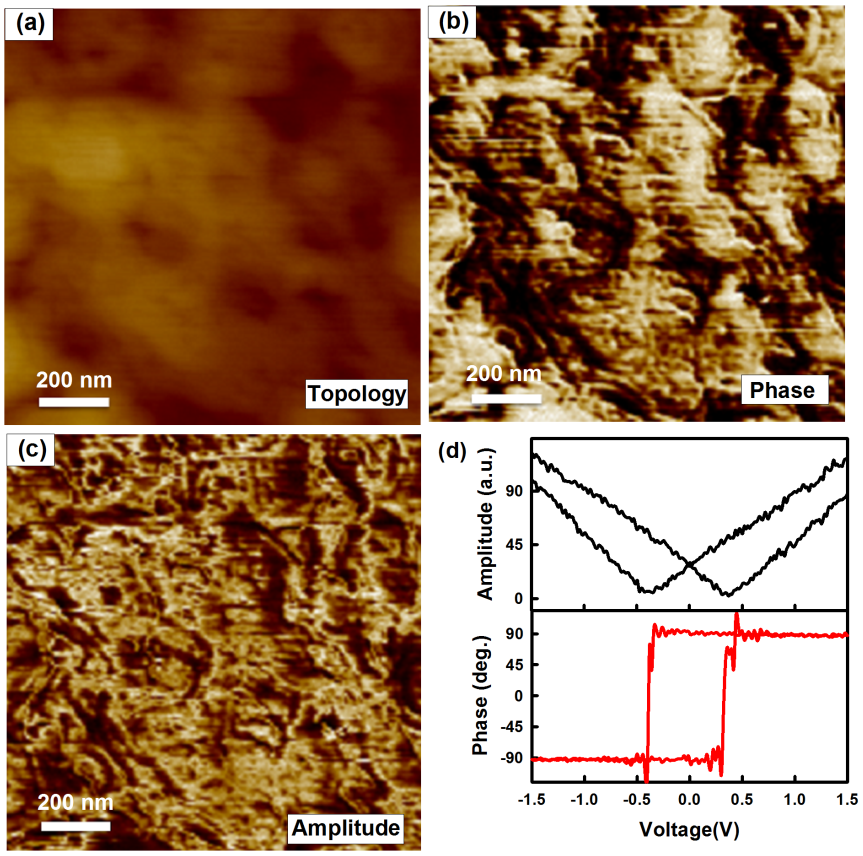

Fig. S9. (a) PFM topology, (b) PFM phase image, and (c) PFM amplitude image of the as-grown $MAPbBr_3$ thin film. (d) Piezoresponse amplitude and piezoresponse phase at different bias voltages.

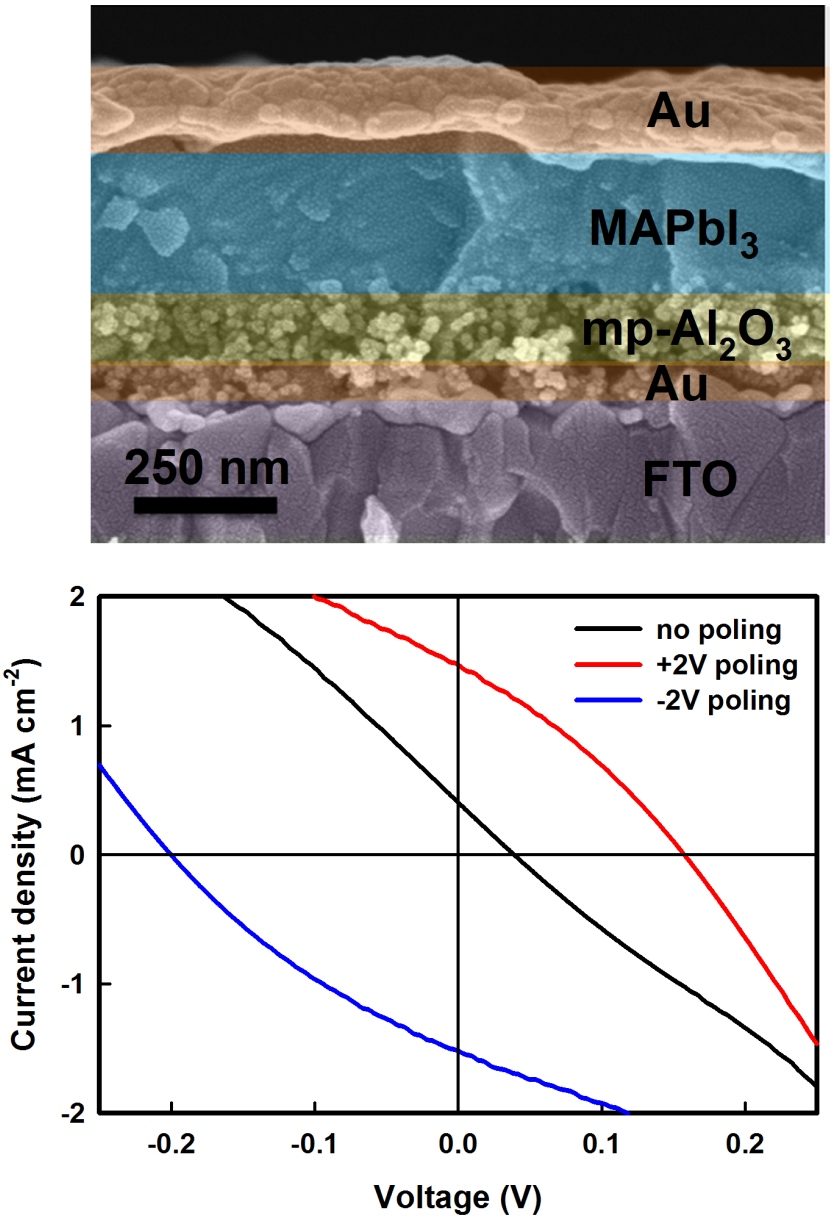

Fig. S10. (a) SEM image and (b) J-V plots of the ferroelectric solar cell with Au/$MAPbI_3$/Au structure.

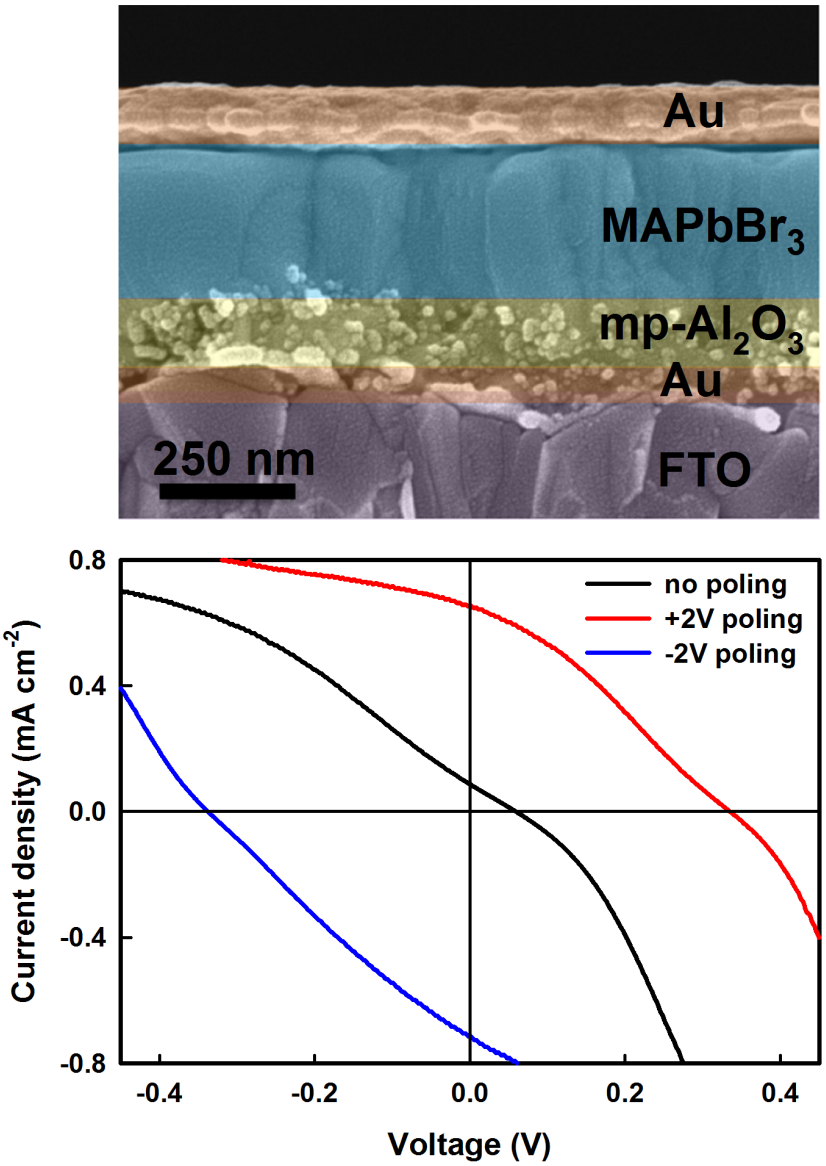

Fig. S11. (a) SEM image and (b) J-V plots of the ferroelectric solar cell with Au/$MAPbBr_3$/Au structure.

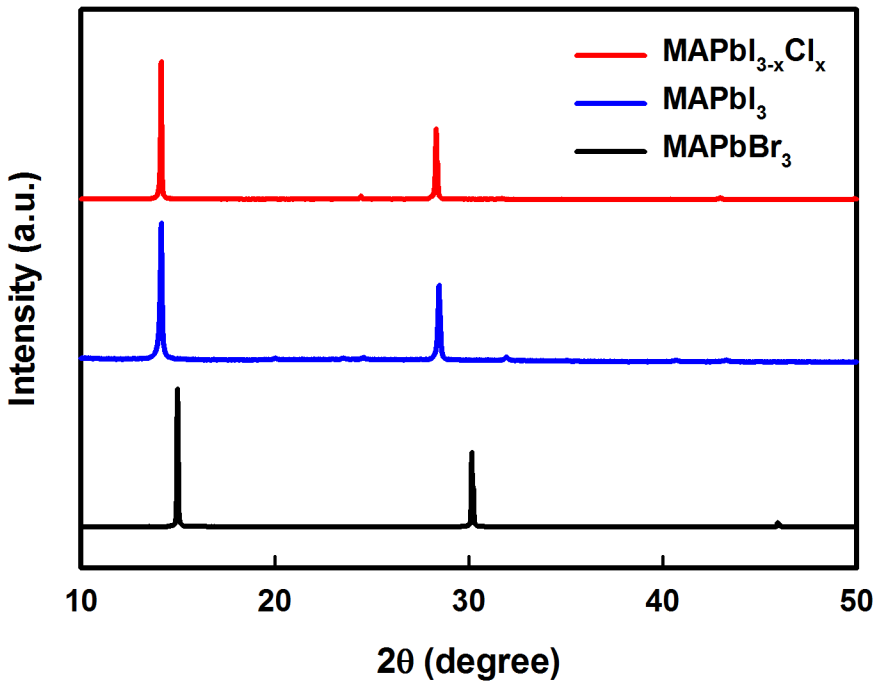

Fig. S12. XRD patterns for the $MAPbI_{3-x}Cl_x$, $MAPbI_3$ and $MAPbBr_3$ thin film on slide glass.

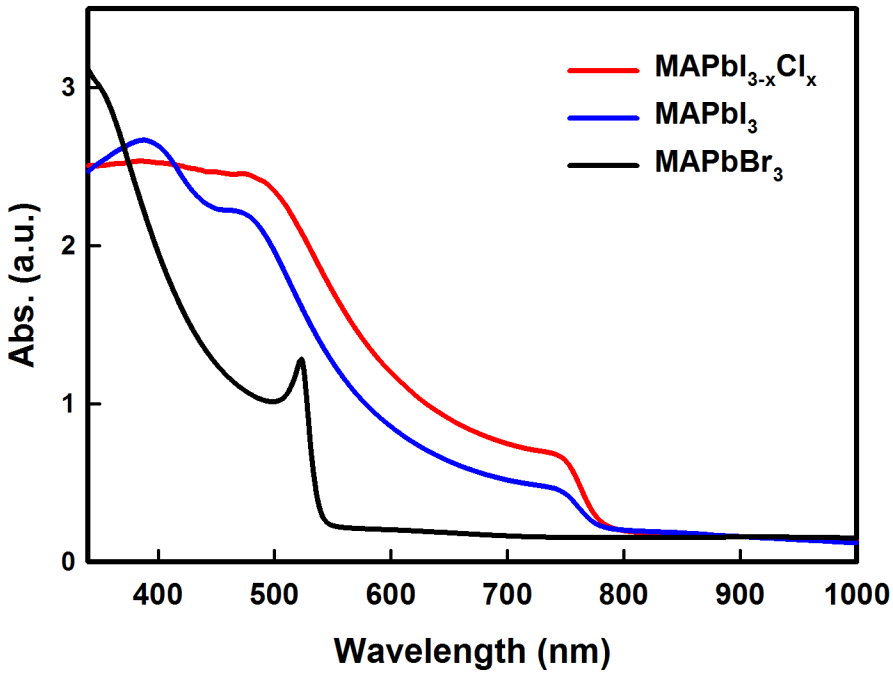

Fig. S13. UV-vis absorption spectra for the $MAPbI_{3-x}Cl_x$, $MAPbI_3$ and $MAPbBr_3$ thin film on slide glass.